Research Square

Preprints are preliminary reports that have not undergone peer review.
They should not be considered conclusive, used to inform clinical practice,
or referenced by the media as validated information.

KW-TB-DSS: A Knowledge-Driven, ExplainableDecision-Support System for UAV-Based Wind-TurbineBlade InspectionKW-TB-DSS: A Knowledge-Driven,Explainable Decision-Support System for UAV-BasedWind-Turbine Blade Inspection

Madhuri Gupta
Bennett University
Harsh S Dhiman
Genpact India Pvt Ltd
Sameer Malik
Worcester Polytechnic Institute
Achyut Shankar
Bennett University
Wattana Viriyasitavat
Chulalongkorn University
Jaydeep Kishore
UPES University
Sonu Kumar Das
sonu.das@jaipur.manipal.edu

Manipal University Jaipur

Article

Keywords: Blade surface, Deep learning, Gradient-weighted Class Activation Mapping, SHapley Additive exPlanations, Wind turbine, Explainable AI

Posted Date: May 18th, 2026

DOI: https://doi.org/10.21203/rs.3.rs-9544675/v1

License: This work is licensed under a Creative Commons Attribution 4.0 International License.
Read Full License

Additional Declarations: No competing interests reported.

KW-TB-DSS: A Knowledge-Driven, Explainable Decision-Support System for UAV-Based Wind-Turbine Blade InspectionKW-TB-DSS: A Knowledge-Driven, Explainable Decision-Support System for UAV-Based Wind-Turbine Blade Inspection

Madhuri Gupta*[a], Harsh S. Dhiman[b], Sameer Malik[c], Achyut Shankar[a], Wattana Viriyasitavat[d], Jaydeep Kishore[e], Sonu Kumar Das[f]

[a]*School of Computer Science and Technology, Bennett University, Noida, Uttar Pradesh, India*
[b]*Assistant Manager, Data & AI, Genpact India Pvt Ltd., Bengaluru, Karnataka, India*
[c]*Worcester Polytechnic Institute, Worcester, Massachusetts, USA*
[d]*Faculty of commerce and accountancy, Chulalongkorn University, Thailand*
[e]*School of Computer Science, UPES University, Dehradun 248007, Uttarakhand, India*
[f]*Department of Business Administration, Manipal University, Jaipur 303007, Rajasthan, India*

Abstract

We present KW-TB-DSS, a knowledge-driven, explainable decision-support system for Unmanned Aerial Vehicle (UAV)-based wind turbine blade inspection. The pipeline (i) preprocesses UAV imagery, (ii) classifies four surface-damage classes using a DenseNet169 backbone, and (iii) fuses pixel-level Gradient-weighted Class Activation Mapping (Grad-CAM) and SHapley Additive exPlanations (SHAP) attributions via kernel ridge regression to generate interpretable heatmaps. Comprehensive experiments on a public aerial blade dataset demonstrate that KW-TB-DSS achieves 97.99% accuracy, 97.43% precision, 96.39% recall, and 96.90% F1-score, outperforming MobileNet and Inception counterparts. Robustness tests under simulated fog (Gaussian blur) show that DenseNet169 maintains a leading accuracy of 79.5%, outperforming Inception (77.1%) and MobileNet (76.2%) de-

*Corresponding author: madhuri.gupta@bennett.edu.in

Email addresses: Madhuri.Gupta@bennett.edu.in (Madhuri Gupta*), hsdhiman1098@gmail.com (Harsh S. Dhiman), smalik@wpi.edu (Sameer Malik), ashankar2711@gmail.com (Achyut Shankar), Wattana@cbs.chula.ac.th (Wattana Viriyasitavat), jaydeep.kishore@upes.ac.in (Jaydeep Kishore), sonu.das@jaipur.manipal.edu (Sonu Kumar Das)

spite notable input degradation. Ensemble attribution maps highlight more trustworthy regions than either Grad-CAM or SHAP alone. By quantifying per-class performance and presenting confusion matrices, the framework ensures balanced detection across all categories of blade damage. In addition, its lightweight design allows seamless integration with Supervisory Control and Data Acquisition (SCADA) dashboards, making it suitable for real-world wind-farm operations. By combining high detection accuracy with operator-ready interpretability, KW-TB-DSS bridges the gap between data-driven prediction and knowledge-enabled decision making, offering a reproducible template for explainable wind-farm maintenance.

Keywords: Blade surface, Deep learning, Gradient-weighted Class Activation Mapping, SHapley Additive exPlanations, Wind turbine, Explainable AI

1. Introduction

Wind power stands out as a leading candidate in the shift toward renewable energy. Wind energy emits almost zero natural pollution [1]. Wind turbines utilize the wind's kinetic energy and transform it into electrical energy. India's installed wind power capacity ranks fourth worldwide after China, the United States, and Germany. Wind energy constitutes nearly 10% of India's electricity demand capacity, which presently accounts for 4% of total power [2]. In 2020-2021, India generated approximately 59.8 TWh of energy using its installed power of 38,785 MW (March 2021) of wind power. Currently, renewable energy sources (excluding large hydro) account for 24.7% of India's total installed power capacity of 382.151 gigawatts (GW). Wind energy comprises 41.5% of the total renewable energy capacity (94,433.4 GW) and is the largest source of pure energy.

As the wind power sector continues its remarkable growth, wind turbine health monitoring is imperative for damage detection and mitigation. However, wind turbines are subject to various damage that could jeopardize their operation, especially in the case of the grid-connected mode. A wind turbine has vulnerable rotating components such as a gearbox, rotor blades, and generator. Potential damage to one of these rotating components can cause a significant reduction in aerodynamic efficiency [3]. Defects and damages can result from manufactur-

ing errors, frequent gusts at the farm site, and asymmetrical rotor hub and blade loading.

$$P = \tfrac{1}{2}\rho A v^3 C_p \tag{1}$$

But you can extend with efficiency loss due to damage:

$$\eta_{\text{damaged}} = \frac{C_p^{\text{damaged}}}{C_p^{\text{ideal}}}, \quad \Delta P = P_{\text{ideal}} - P_{\text{damaged}} \tag{2}$$

This quantifies how surface roughness changes C_p. All these factors contribute to the reduction in aerodynamic efficiency of the wind turbine. When turbine blades are affected by surface pollutants—including rust, oil, dust, ice, and insect remains—the actual energy output can fall to nearly 40% of the nominal capacity. Moreover, literature reports that operation and maintenance may comprise up to 30% of the total expenditure in wind energy systems[4]. Wind turbine edges show a unique challenge, and numerous edge damages can occur throughout a wind turbine. Edge and surface damage to turbines is likely the most expensive in terms of O&M expenses. Most of the turbine's force is generated at the leading edge and cutting-edge ends. In this case, it is imperative to adopt a condition-monitoring framework that continuously assesses the health of turbine blades [5]. We term our proposed framework KW-TB-DSS (Knowledge-Driven Turbine Blade Decision-Support System). The rationale for this naming is twofold: (i) the framework is knowledge-driven in the sense that it does not stop at classifying blade surface damages but further transforms raw UAV imagery into actionable operator knowledge through explainable outputs (Grad-CAM and SHAP heatmaps) and ensemble fusion; and (ii) the framework is decision-support oriented, designed to supplement wind farm operators in maintenance scheduling, compliance monitoring, and early fault diagnostics. By combining deep learning with ensemble XAI, KW-TB-DSS provides both high detection accuracy and interpretable reasoning at the pixel level, bridging the gap between data-driven predictions and knowledge-enabled decision making. This dual focus ensures that the system not only detects erosion and surface damage reliably but also explains its predictions in a form that

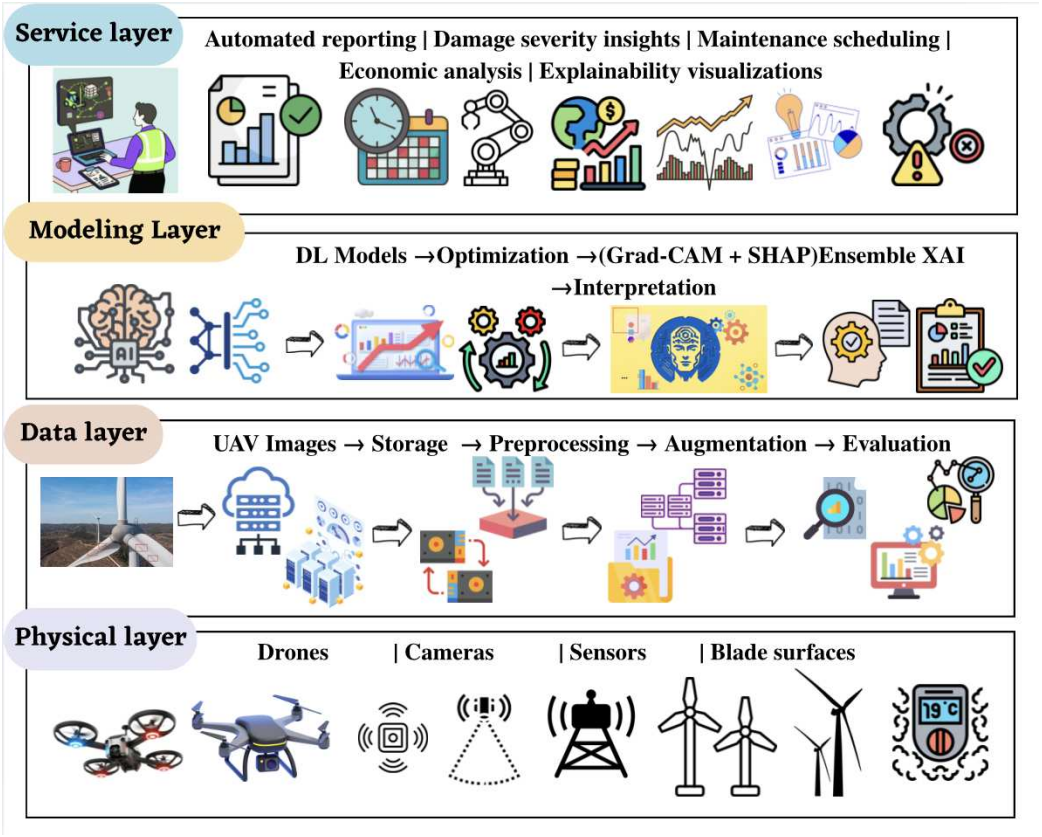


Figure 1: Four-Layer Architecture of the Proposed KW-TB-DSS Framework

is directly usable for practical inspection and operational workflows. To provide a high-level view of the proposed inspection and decision-support system, Figure 1 summarizes the four-layer architecture underlying KW-TB-DSS, from physical data acquisition to operator-oriented services. Table 1 illustrates the impact of blade surface damage on performance and cost.

1.1. Related work

A commonly used vibration-based technology is a potential solution to address fault detection and health monitoring of the gearbox, generator, and rotor blades. The vibration-based approach is often supplemented with signal processing techniques such as Fourier analysis, wavelet transform (WT), and empirical

Table 1: Impact of Wind Turbine Blade Surface Damage on Performance and Costs

S.N.	Parameter	Reported Effect
1	Power loss due to surface roughness	Up to 40% reduction in actual energy output
2	Contribution of surface/edge damage to turbine failures	Approximately 20% of total failures
3	O&M cost proportion in total expenditure	Up to 30%
4	Leading-edge & cutting-edge criticality	Major contributor to aerodynamic efficiency
5	Economic risk	High repair/replacement cost + downtime

mode decomposition (EMD), which aids in the accurate distinction of healthy and faulty vibration signatures acquired from the rotating components [6, 7]. Implementing a condition monitoring framework specifically designed to manage a wind turbine's sensitive equipment could enhance the wind turbine's efficiency, maintenance, and downtime costs. Thus, this approach enables the development of a condition monitoring and fault diagnosis framework for wind turbines, supporting operators in making informed decisions [8, 9]. Researchers across multiple domains have proposed computational methods that learn system behavior from historical data to enhance predictive analysis[10, 11, 12].

Advanced learning algorithms are increasingly employed to model and forecast the time-series dynamics of key turbine indicators, including gearbox oil properties and bearing temperature[13]. Apart from gearbox, yaw systems for wind turbines have been studied extensively from an O&M point of view [14, 15]. For a wind turbine, the focus is safety, maintainability, availability, and reliability. To avoid catastrophic damage scenarios in a specific wind farm, the primary condition-monitoring job for this article is the recognition of wind turbine blade surface damage. Blade defects account for a considerable proportion of failures, contributing to nearly 20% of the issues encountered throughout the operational lifetime of a wind farm[16]. High-resolution photographs captured by a drone or manual inspection detect potential damage, and a one-year study of edge defor-

mation follows this process. In the worst possible case, however, an edge failure may necessitate significant costs to repair or replace an existing blade, increasing wind turbine downtime. Further, information extracted from a damaged wind turbine blade in the form of high-resolution images. It requires significant storage space, manual assessment, and annotation of their respective damage categories. Automating the damage detection process of wind turbines means dropping the on-site working man, whereas skilled labor is required to operate and navigate the aerial vehicle.

There are numerous strategies for monitoring the condition of a wind turbine's sensitive rotatory and non-rotating components. In [17], a diagnostic approach for assessing turbine blade health is introduced, utilizing a system of high-fidelity optical sensors integrated with wireless sensor networks (WSNs). Field measurements are conducted in which multivariate data from sensory circuits is transmitted to verify its veracity. Another approach for condition monitoring and damage localization in wind turbine blades is introduced, based on frequency response transmissibility in [18]. The technique employs the condition monitoring (CM) signals estimated by adjacent wind turbine sensors. Results demonstrate precise damage detection and location. However, this method is inadequate for detecting ice and snow accumulation on wind turbine blades. In [19], micro-electromechanical systems (MEMS) sensors are utilized in the damage expectation of edges, which address worldwide observing methodology where the entirety of the edge is under investigation.

The literature is limited to machine vision for detecting surface damage on wind turbine blades. Machine vision-based maintenance routine enables detection of external turbine blade damages such as cracks, blade edge erosion, and scratches [20]. With machine vision-based techniques, issues like accessibility and potential safety risks can be eliminated [21, 22]. Wang et al. utilized drone images for crack detection in wind turbines. To pre-process the raw input data, authors implemented Haar-like features [23]. The classification technique is chosen from a set of base algorithms, namely, Support Vector Machine, Decision Tree,

and LogitBoost. However, the work is limited to detecting the damage to the turbine blade. It is based on explainable models, which determine the accuracy level for a crucial problem like damage detection. In [23], a technique for the location of surface breaks in wind turbine edges based on unmanned aerial vehicle (UAV) images is proposed.

Astolfi et al. discussed explainable AI (XAI) techniques for condition monitoring of wind turbines and noted limitations while modeling wind turbine power curves via univariate approaches [24]. XAI techniques, such as Shapley coefficients, are used to identify and monitor variables affecting wind turbine performance. Chatterjee et al. presented a Recurrent Neural Network (RNN) and XBoost-based hybrid anomaly detection framework that explains the importance of features involved in the condition monitoring process [25]. In [26], authors have discussed machine learning algorithms and meteorological variables to predict daily energy production. The Shapley additive explanations algorithm reveals the individual contributions of meteorological factors to predictions, with wind speed emerging as the most influential variable, followed by turbulent kinetic energy. In [27, 28], Chatterjee et al. discussed a framework utilizing XAI for wind turbine O&M using SCADA data. The framework also talks about generating alarm messages using natural language processing (NLP) based on the operational state of the wind turbine. The work also extends to studying the behavior of the onshore wind turbines without learning additional features via the transfer learning approach. In [29], authors discuss their key findings from the project titled “XAI4Wind", where a multimodal Knowledge Graph (KG) for wind turbine O&M is introduced. The KG deals with wind turbine information through multivariate SCADA data, images, and alarm logs. In [30], to determine the position and severity of stator inter-turn faults (ITFs), fault types, and IM health status of wind turbines, the author proposed three convolution neural network (CNN) CNN-based deep Learning (DL) models such as Inception, Xception, and MobileNet. Spatial-time-frequency features are produced by merging deep features from various CNNs using the discrete wavelet transform (DWT).

This fusion increases diagnostic accuracy while decreasing the size of the input characteristics. Yajuan et al. [31], Wind Turbine blade surface damage detection based on lightweight deep learning network. In this work, researchers have used Mobiile Net and YOLOv3. The findings show that the detection approach suggested in this article has a mean average precision (mAP) of over 90 percent and a detection speed of around twice as fast as YOLOv3-DarkNet53. The benefits of this approach are low bandwidth use, great accuracy, and quick detection speed. In [32], the researcher applied a deep neural network called Mask-MRNet to identify wind turbine blade faults using images of unmanned aerial vehicles. DenseNet-121 is selected as a classification model for Mask-MRNet. As per the study, DenseNet is preferable to select the classifier under particular application requirements.

1.2. Contributions of this work

In this manuscript, we discuss the blade surface damage detection of wind turbines using aerial imagery and deep learning framework in tandem with XAI. Deep learning and computer vision appear to be well-developed fields that significantly contribute to wind turbine predictive maintenance. As a result, we have attempted to address the problem of blade surface damage detection in this publication by developing a multi-class classification system based on image analytics. The benefits of image analysis-based blade health maintenance include (i) less human effort in terms of man hours at the wind farm site, (ii) regular turbine observation, and (iii) accurate information extraction via aerial photography. With aerial imagery-based data capture of wind turbine blades, human errors that might otherwise delay turbine inspection may now be readily handled. The idea behind XAI for wind turbine blade damage detection is to bring accountability, transparency, and operator trust. A significant advantage of using XAI with fault detection is monitoring compliance and regulatory standards of the crucial wind turbine equipment such as rotor blades, gearbox, generator, and yaw system. The XAI-generated results, such as heatmaps and importance scores, can strengthen the reasoning behind a particular prediction, thus ensuring a seamless integration

of XAI with the deep learning predictions for wind turbine blade damage. Overall, explainable fault detection of wind turbine blades can supplement wind farm operators to investigate root causes for catastrophic blade damages and raise early warning alarms. The main contributions of this research work can be summarized as follows:

1. UAV-Based Multi-Class Damage Detection: We design a deep learning framework that leverages UAV-acquired imagery for four-class blade surface damage detection. Pre-processing and image augmentation address data imbalance and improve training quality. Multiple CNN-based transfer learning models (MobileNet, Inception, and DenseNet169) are evaluated, with DenseNet169 achieving the best overall performance.
2. Explainable and Robust Predictions: To enhance transparency and trust, we integrate Grad-CAM and SHAP explainability techniques, which highlight pixel-level regions influencing model predictions. An ensemble fusion of Grad-CAM and SHAP further strengthens interpretability. In addition, a sensitivity analysis under augmentation and Gaussian blur validates the robustness of the DenseNet169 model in uncertain visual conditions.
3. KW-TB-DSS: Operator-Centric Decision Support: We introduce KW-TB-DSS (Knowledge-Driven Turbine Blade Decision Support System), which unifies UAV imagery, deep learning, and ensemble explainability into an operator-ready decision-support framework. Beyond classification, the system provides interpretable, trustworthy insights to aid compliance monitoring, maintenance planning, and early warning of catastrophic blade damages.

The remainder of the manuscript is organized as follows: Section 2 discusses deep learning techniques for the proposed problem. In Section 3, the wind turbine blade image dataset is described along with the importance of image augmentation. In Section 4, the results of numerical simulation for turbine blade damage detection are presented, followed by sensitivity analysis. In Section 5, conclusions are discussed.

2. Computer Vision-aided Deep Learning Framework

Artificial intelligence's computer vision field focuses on visual analysis and inquiry to aid decision-making. It is frequently utilized in industrial components and systems for supervision, facial identification, and medical diagnosis. In this instance, a deep learning framework based on computer vision is suggested for detecting surface degradation on wind turbine blades. Drone photographs of wind turbine blades have excellent clarity. Further analysis is performed on these high-resolution images to identify significant features. To solve the problem of turbine blade surface damage detection, a computer vision-based deep learning framework can be adopted. MobileNet, DenseNet169, and Inception deep learning models are incorporated in the research work. The MobileNet architecture used

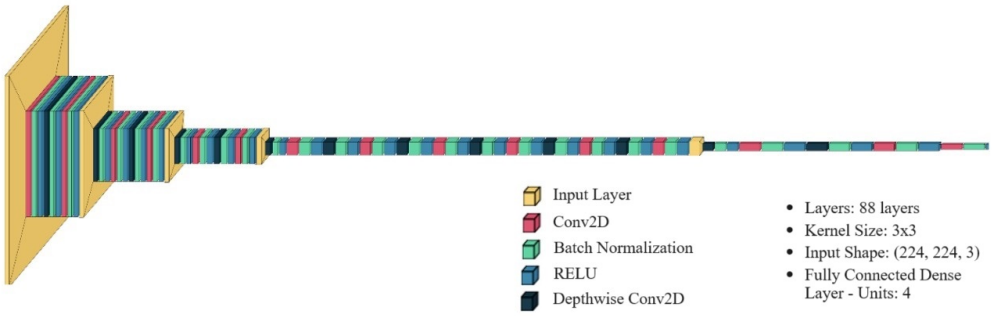


Figure 2: MobileNet architecture for wind turbine blade damage detection

in this model has 88 layers with a 3x3 kernel size. The input shape is assumed to be (224, 224, 3), the standard input shape for the MobileNet architecture. The architecture utilizes the final five layers of the pre-trained MobileNet model as input features, followed by a fully connected dense layer comprising four neurons with softmax activation for classification. The model is trained using the Adam optimizer and sparse categorical cross-entropy loss, with accuracy selected as the performance metric. The last 22 layers are frozen during training to avoid overfitting, as shown in Figure 2.

The convolutional layer output is given by:

$$z_{i,j}^{(l)} = \sigma\left(\sum_{m,n} W_{m,n}^{(l)} \cdot x_{i+m,j+n}^{(l-1)} + b^{(l)}\right)$$

where (i, j) are pixel coordinates, W are kernel weights, and σ is the activation function.

For multi-class classification, we use softmax:

$$\hat{y}_i = \frac{e^{z_i}}{\sum_{j=1}^{C} e^{z_j}}, \quad i = 1, \ldots, C$$

The training objective is categorical cross-entropy:

$$\mathcal{L}_{CE} = -\sum_{i=1}^{C} y_i \log \hat{y}_i$$

Optimization with Adam is expressed as:

$$m_t = \beta_1 m_{t-1} + (1 - \beta_1) g_t, \quad v_t = \beta_2 v_{t-1} + (1 - \beta_2) g_t^2$$

$$\theta_{t+1} = \theta_t - \alpha \cdot \frac{m_t / (1 - \beta_1^t)}{\sqrt{v_t / (1 - \beta_2^t)} + \epsilon}$$

Algorithm 1 depicts a step-by-step approach for Gaussian blur

2.1. Model parameters

The model parameters for baseline CNN, DenseNet169, Inception, and MobileNet can be summarized in the following Table 2. The implemented deep learning architecture is designed to classify images into four possible classes. To extract pertinent features from the input images, the model uses a pre-trained DenseNet169 Convolutional Neural Network as illustrated in Figure 3. Subsequently, two fully connected layers, a global average pooling layer, batch normalization, and dropout are incorporated, followed by a dense classification layer with

Algorithm 1 Gaussian Blur Algorithm

procedure GAUSSIANBLUR(Image I, Kernel size k, Standard deviation σ)
    $G \leftarrow$ GenerateGaussianKernel(k, σ)
    $I_{\text{blurred}} \leftarrow$ Convolve(I, G)
    return I_{blurred}
end procedure
procedure GENERATEGAUSSIANKERNEL(Kernel size k, Standard deviation σ)
    $G(x, y) \leftarrow \frac{1}{2\pi\sigma^2} \cdot e^{-\frac{x^2+y^2}{2\sigma^2}}$
    return G
end procedure
procedure CONVOLVE(Image I, Kernel K)
    $I_{\text{convolved}}(i, j) \leftarrow \sum_m \sum_n I(m, n) \cdot K(i - m, j - n)$
    return $I_{\text{convolved}}$
end procedure

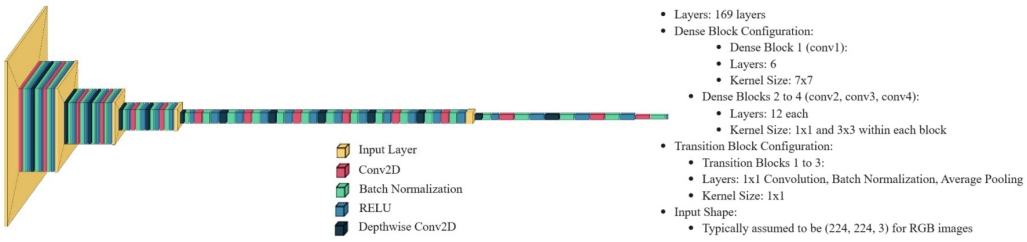


Figure 3: DenseNet169 architecture for wind turbine blade damage detection

four neurons and softmax activation. To balance generalization and adaptation, only the final eight layers of the base network are fine-tuned, while the preceding layers remain frozen to retain pre-trained representations. The model is optimized using Adam with categorical cross-entropy loss and accuracy as the evaluation metric, employing transfer learning to enhance classification performance.[33, 34]. The Inception model has convolutional layers that use kernel sizes of 1 x 1, 3 x 3, and 5x5, and max-pooling layers with a pool size of 3 x 3 and a stride of 2. The global average pooling layer computes the mean of each feature map. The dense layers have 1024 and 4 units, respectively, with ReLU and softmax activation functions. The model takes a 4D tensor of shape (batch size, height, width,

Table 2: Model parameters

Parameter	Value
Input image size	$224 \times 224 \times 3$ pixels
Number of classes	4
Batch size	64
Epochs	100
Learning rate	0.001
Optimizer	Adam
Loss function	Categorical cross-entropy

channels) as input. Overall, the model architecture combines convolutional, pooling, and dense layers with various kernel sizes to extract features from images and classify them into specific categories, as shown in Figure 4 [35].

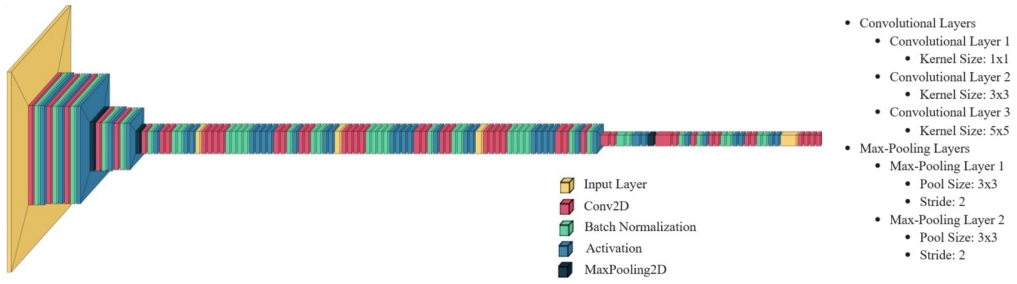


Figure 4: Inception architecture for wind turbine blade damage detection

2.2. Ensemble Explainable AI Models

Artificial Intelligence (AI) has advanced significantly over the past ten years, which has led to the use of algorithms for a wide range of problem-solving applications. To achieve this accomplishment, more complicated models and opaque black-box AI models have been used. XAI has been offered as a solution to this problem to increase AI's transparency and promote its acceptance in essential fields. With the advances in deep learning-based models, the call for explainability of such methods expands, especially in image pattern identification. Explainable AI (XAI) refers to the ability of an AI system to make its predictions and

potential biases understandable. It plays a vital role in ensuring model validity, fairness, transparency, and interpretability of AI-driven decisions. For successful deployment, organizations must provide clear explanations of AI behavior to build stakeholder trust. Incorporating explainability further supports the adoption of responsible and ethical AI development practices. Ensemble methods are frequently used in deep learning due to their capacity to reduce bias and variation and, hence, increase reliability [36]. The stacking-based ensemble method is popular in deep learning studies for imaging and has demonstrated effectiveness in several of them [37, 38, 39]. We suggest an ensemble method for image interpretation based on stacking that utilizes the results of the primary interpretation method. It would be interesting to know whether using both methods simultaneously produces complementing gains, as the Grad-CAM [36] and SHAP [37] gradient explainer methods are both gradient-based algorithms with unique mechanics but similar benefits. To test this hypothesis, we propose an ensemble framework that constructs a mapping layer capable of highlighting discriminative regions by integrating Kernel Ridge Regression with normalized Grad-CAM outputs and normalized positive SHAP values. This approach is known as Ensemble XAI.

2.3. GradCAM

Grad-CAM: This approach calculates the gradients of the output $f_c(x)$ w.r.t. feature map activations A_k of a specified layer [37]. The important weights are then calculated by averaging the gradients for each channel k (along with width W and height H):

$$a_k^c = \frac{1}{H \cdot W} \sum_{i=1}^{W} \sum_{j=1}^{H} \frac{\partial f_c}{\partial A_{ij}^k} \cdot x \tag{3}$$

As a result, the layer activations are multiplied by the average gradient for each channel, a_k, and the results are added for all channels. Bilinear interpolation can be used to upsample the Grad-CAM output to the input image resolution after a

ReLU is applied to the production, which only returns non-negative attributions:

$$\Theta\text{Grad-CAM}(f_c, x) = \text{UPSAMPLE}_{\text{Bilinear}}\left(\text{ReLU}\left(\sum_k a_k^c A^k\right)\right) \tag{4}$$

Grad-CAM intuitively emphasizes rough areas of the image that positively contribute to $f_c(x)$. Grad-CAM weights are normalized as:

$$\tilde{A}^k = \frac{A^k - \min(A^k)}{\max(A^k) - \min(A^k)}$$

2.4. SHAP

SHapley Additive exPlanation (SHAP) is a well-known XAI system that can offer model-independent local explainability for tabular, image, and text datasets [28]. This technique explains individual predictions by leveraging Shapley values, a concept grounded in cooperative game theory. A Shapley value quantifies the average marginal contribution of a given feature across all possible feature value combinations within the input space. Shapley values is a widespread technique from cooperative game theory with some good qualities. The feature values of a data instance play as performers in a coalition. The average marginal contribution of a feature value to overall potential coalitions is the Shapley value. SHAP values are defined by:

$$\phi_i(f, x) = \sum_{S \subseteq N \setminus \{i\}} \frac{|S|!(|N| - |S| - 1)!}{|N|!}\big[f(S \cup \{i\}) - f(S)\big]$$

Approximation with sampling is:

$$\phi_i \approx \frac{1}{M}\sum_{m=1}^{M}\big[f(x_{S_m \cup \{i\}}) - f(x_{S_m})\big]$$

3. Methodology & Data Description

An aerial image–driven deep learning model for identifying turbine blade erosion is presented in Figure 5. It is the proposed KW-TB-DSS methodology framework. The pipeline consists of UAV data acquisition, annotation, preprocessing and augmentation, deep learning classification, XAI-based interpretability, evaluation (robustness and performance), and decision support for turbine maintenance planning and economic analysis. The UAV acquires high-resolution images of

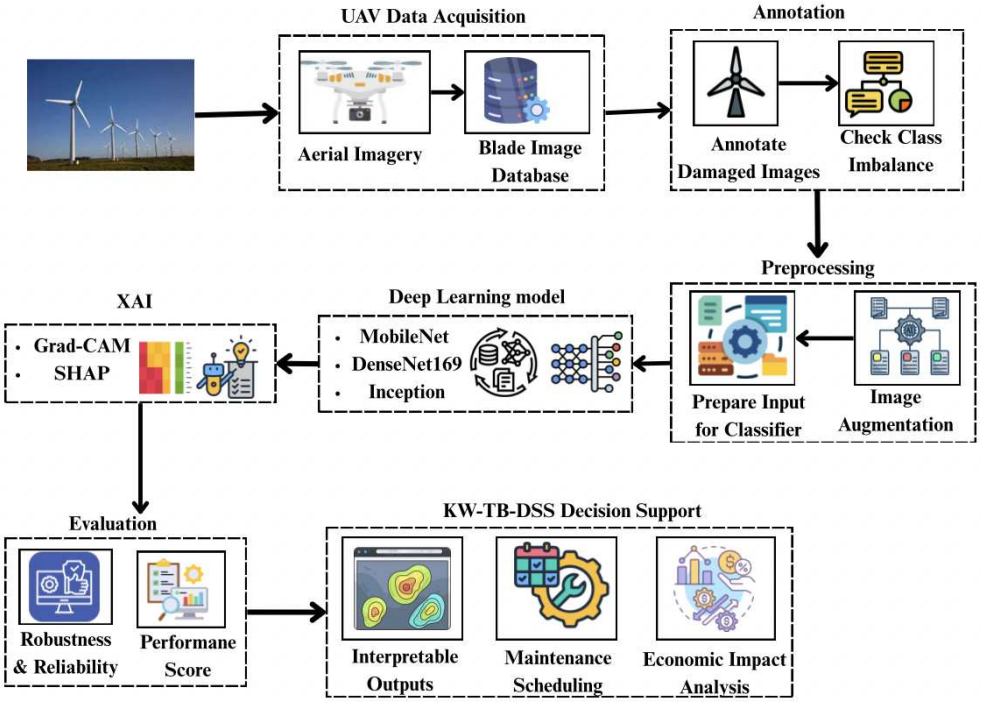


Figure 5: Aerial Imagery, Deep Learning, and Ensemble XAI-based Wind Turbine Blade Erosion Detection Framework

turbine blades and transmits them wirelessly to a central server for further processing. These images with varied damage severity indicate potential classes or labels in the case of a supervised learning framework. The next step is manual annotation of the images collected via a UAV. The interference of human aid to

the digitally collected turbine blade images makes this entire framework reliable and efficient. Manual annotation of collected images is followed by assessing the class imbalance, where the disparity in the number of images collected is visualized in the form of a histogram. Image augmentation enables image transformation via scaling, cropping, filtering, rotation, padding, and flipping. The objective of such an augmentation procedure is to inject variety in the image dataset, thus not polluting the original dataset and enhancing the quality of the deep learning training procedure. Once the input images are ready, a deep learning-based image classifier is used to determine the label/class of the given image. In this framework, the label/class indicates the type of blade damage. Performance score, as shown in Figure 5, could be accuracy, recall, and precision, demonstrating the effectiveness of the proposed model. Once a performance score is calculated, the recommendation engine gives qualitative insights to the wind farm operator. For a given wind farm under consideration, the blade damage could result in power reduction over a while. This power reduction can cause a significant loss in revenue to the wind farm operator. Thus, from an economic perspective, implementation of such a condition monitoring framework is imperative. In line with the system-oriented perspective of this work, the proposed framework is formalized as KW-TB-DSS (Knowledge-Driven Turbine Blade Decision-Support System). The methodology is structured into three layers: (i) a data layer, where UAV imagery is acquired, pre-processed, annotated, and augmented to ensure robust training data; (ii) a modeling layer, where deep learning architectures such as MobileNet, DenseNet169, and Inception are applied for multi-class blade damage detection, with explainability achieved through Grad-CAM and SHAP fusion; and (iii) a decision-support layer, where interpretable outputs, confidence estimates, and aggregated knowledge are presented in a dashboard format. This final layer links AI-driven analytics with actionable guidance, enabling operators to plan inspections, schedule repairs, and estimate economic impacts. By structuring the methodology as a complete decision-support pipeline, KW-TB-DSS bridges the gap between data-driven fault detection and practical wind-farm operations. Figure 6 illustrates

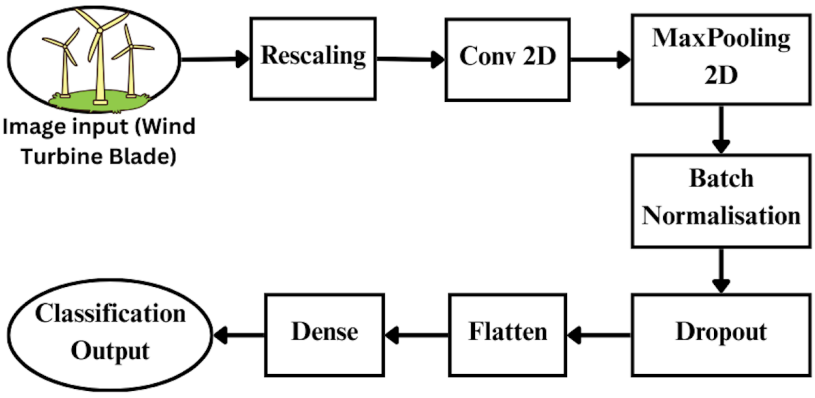


Figure 6: Low-level schematic for wind turbine blade damage detection

a low-level schematic for wind turbine blade damage detection involving the use of a deep learning architecture with re-scaling, 2D convolutional, max-pooling, batch normalization, and dense layers for final classification. In this paper, deep learning architectures are built around these layers with different configurations, thus resulting in different classification performances. The dataset utilized in this research is obtained from Mendeley and consists of drone inspection images of a wind turbine [40]. A total of four categories, namely, erosion area, damaged area, edge area, and reference area, are considered in this study. Figure 7 illustrates the types of surface damage for a wind turbine blade.



Figure 7: Types of surface damages for wind turbine blade

The dataset is a valuable resource for testing and evaluating structure from motion (SFM) algorithms, which are vital for 3D reconstruction tasks. Moreover, it serves as a base dataset for machine learning algorithms aiming to identify damaged areas along edges or assess the roughness of edge surfaces in this study. The images in the dataset were captured using Canon's 5Ds DSLR high-resolution camera, with an impressive resolution of 8688×5792 and utilizing a three-channeled RGB color profile. This dataset consists of four wind turbine blade patches with varied surface defect intensities, namely, the damaged region, erosion region, edge defect, and a reference region that does not contain any roughness or damage. The original dataset consists of images in limited quantity, and hence, the classification approach suffers from the problem of class imbalance. To solve this, an image augmentation approach is adopted. Augmentation can be utilized to increase the size of the training dataset by changing the properties of an image. Literature reveals that for a classification task on a larger dataset, deep learning techniques can yield meaningful models, with augmented data enhancing the performance of the overall framework. In this manuscript, we have used the augmentation properties as follows-

1. Height shift and width shift are used to introduce variation in the height and width of an input image. This adjusts the height and width by a random factor.
2. Rotation is used to rotate an image with a factor, often a multiple of 2π, thus rotating the image in a clockwise direction.
3. Horizontal flip and vertical flip are used to flip an input image to generate new variations in the training dataset.
4. Zoom range is used for zooming. An input image can be zoomed in or out on each axis independently.
5. Brightness and Contrast are used to randomly change the brightness and contrast level of an input RGB image and require a factor to be passed as an argument.

Figure 8 illustrates the blade images where different types of augmentation prop-

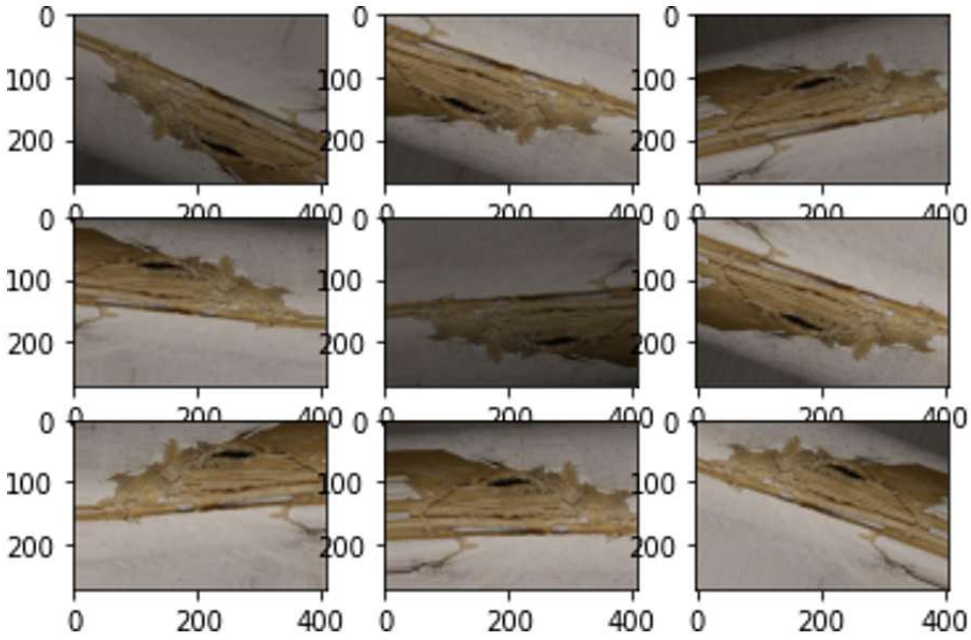


Figure 8: Blade images with different types of augmentation properties

erties, as discussed above, are implemented. Figure 9 represents the number of images used in the training and validation phase for other damage classes. The training-to-testing ratio can also impact the performance of the deep learning classifier.

4. Experimental Results

The training process took place on a system equipped with an Intel Core i5-4570 CPU operating at 3.20 GHz and with 8 GB of memory. The implementation was implemented using Python 3.8 on the Windows 10 operating system. The objective of the proposed framework is to address the damage detection capability of four deep learning-based algorithms, namely, MobileNet, DenseNet169, and Inception. The algorithms are initially trained over images from which meaningful features are extracted and processed further to obtain performance metrics. Two explained Artificial Intelligence models, such as Grad-CAM and SHAP, are

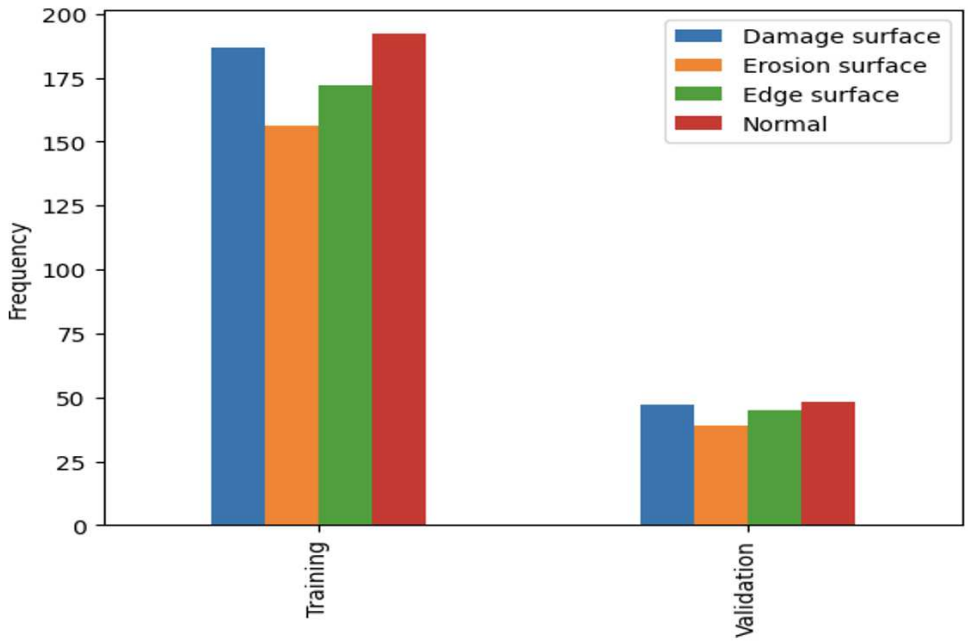


Figure 9: Number of images used in the training and validation phase

incorporated to enhance the expandability of the models. In the context of deep learning, it is crucial to have a representative dataset comprising thousands of training samples to create an effective detection model. However, the images captured by drones have a large size of 8868 × 5792 pixels, making them unsuitable for direct use in training deep learning models and hence are resized to 224×224 pixels. To enable accurate model training, the images belonging to all the classes were resized, annotated (classified) based on their respective damage categories, and augmented. This process was also applied to the remaining classes to ensure uniformity and enhance the overall training process. As a result, the dataset was better prepared for training the deep learning model effectively. Augmentation techniques transform the base images obtained during aerial inspection to cope with the class imbalance problem for wind turbine blade images. To evaluate our

trained model, the following metrics are used:

$$\text{Precision} = \frac{\text{TP}}{\text{TP} + \text{FP}},$$
$$\text{Sensitivity (\%)} = \frac{\text{TP}}{\text{TP} + \text{FN}},$$
$$\text{F1-Score} = \frac{2 \times \text{Precision} \times \text{Recall}}{\text{Precision} + \text{Recall}},$$
$$\text{Accuracy (\%)} = \frac{\text{TP} + \text{TN}}{\text{TP} + \text{TN} + \text{FN} + \text{FP}} \times 100.$$

Here, TP, TN, FP, and FN denote True Positive, True Negative, False Positive, and False Negative values, respectively, in the confusion matrix.

4.1. Baseline comparison

A baseline comparison of DenseNet169 deep learning architecture is carried out with Inception and MobileNet to establish the effectiveness of the proposed framework. The model parameters for these deep learning architectures are derived from previous works carried out [30, 31, 32]. Results reveal that DenseNet169 performs the best when compared with Inception, MobileNet, and a baseline CNN architecture. As far as precision and recall metrics are considered, the average of all the respective damage classes is computed. DenseNet169 yields the maximum precision value and comparable value for recall parameters with other models. Table 3 depicts the performance metrics for turbine blade damage detection for the image classifiers considered.

Table 3: Performance Metrics for Blade Surface Damage Detection

Classifier	Accuracy (%)	Precision (%)	Recall (%)	F1-score (%)
Inception	96.4	96.25	96.10	96.17
DenseNet169	97.99	97.43	96.39	96.90
MobileNet	95.46	95.40	95.39	95.39
Baseline CNN	85.47	84.92	84.36	88.23

The ability of DenseNet169 to accurately identify blade surface damage(s)

makes it an ideal candidate for real-time deployment. Given a wind farm with many wind turbines, manual inspection is time-consuming and often causes increased turbine downtime. With the proposed deep learning techniques, DenseNet169 delivers an excellent detection performance with its ability to extract high-level features. However, the current framework faces certain limitations regarding types of surface damage for a given turbine. Moreover, this model performs well only for a given turbine blade dataset and needs to be tuned further based on the variety of images collected during the aerial inspection phase. Further, to validate the superior performance of DenseNet169, blur wind turbine blade conditions are fed, and performance metrics are computed as listed in Table 4. The images of the

Table 4: Performance Metrics with Gaussian blur

Classifier	Accuracy (%)	Precision (%)	Recall (%)	F1-score (%)
Inception	77.10	76.90	77.60	77.10
DenseNet169	79.5	79.32	79.55	79.20
MobileNet	76.21	75.23	76.29	76.25

wind turbine blades are corrupted with Gaussian blur with varying intensity and are further subjected to augmentation, as discussed in the previous section. The non-blur image is convolved with the Gaussian kernel, and the resulting image consists of finer details. In the present case, a 2D Gaussian kernel function is used as follows:

$$G(x, y) = \frac{1}{2\pi\sigma^2} \cdot e^{-\frac{x^2+y^2}{2\sigma^2}}, \tag{5}$$

where x and y denote the pixel coordinates of the given image in the 2D space, and $G(x, y)$ refers to the image intensity after applying Gaussian blur. Further, a given image I is convolved with kernel K as follows

$$(I * K)(i, j) = \sum_m \sum_n I(m, n) \cdot K(i - m, j - n), \tag{6}$$

where m and n indicate the image indices to generate[41]. In frequency space,

Gaussian filtering is:

$$\hat{I}(u,v) = \hat{I}_0(u,v) \cdot e^{-\frac{u^2+v^2}{2\sigma^2}}$$

Figure 10 illustrates eroded blade images with Gaussian blur. In the figure, the

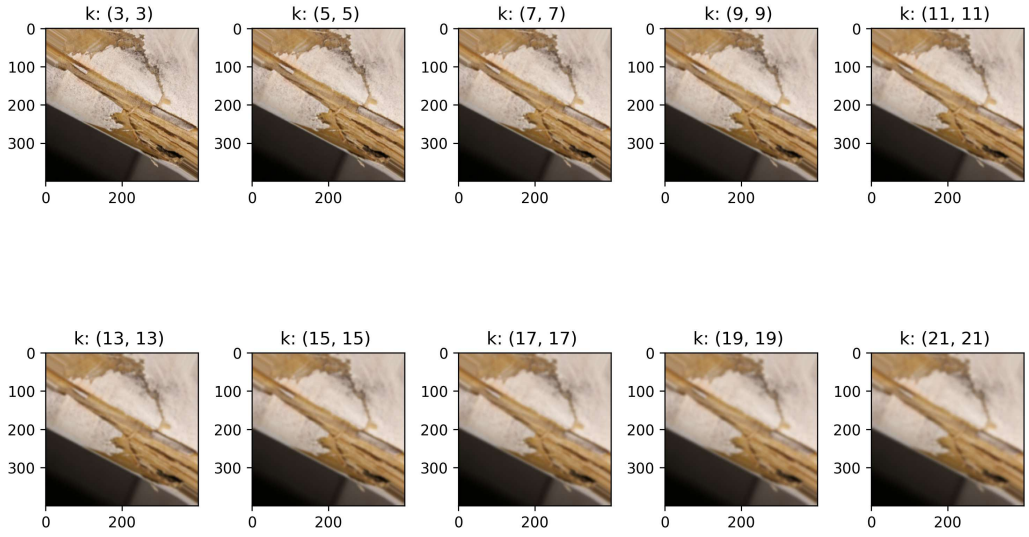


Figure 10: Wind turbine blade images with erosion damage corrupted with Gaussian blur

k value indicates the kernel size of the filter. It can be illustrated that with increasing kernel size, the blur intensity for the images increases. For this experiment, all four image classes are treated with Gaussian blur and are classified into their respective classes as depicted in Table 4. DenseNet169 yields a maximum accuracy of 79.5%, followed by Inception and MobileNet with 77.10% and 76.21%. DenseNet169 allows an efficient flow of information among the succeeding convolutional layers and thereby learns better. However, regarding scalability, DenseNet may face significant challenges like increased memory requirement and computational complexity due to the dense connectivity of the network. On the other hand, Inception architecture can handle large volumes of training data by enabling parallel processing of high-level features at different scales.

4.2. Sensitivity Analysis

The damage detection framework in this manuscript focuses on three image classification techniques. Further, with the help of image augmentation, it is possible to improve the image quality of the turbine blade dataset. In this section, a sensitivity analysis is performed by varying the image augmentation attributes, as discussed in the previous section.

Table 5: Effect of Image Augmentation on DenseNet169 Performance

Sr No	Image Augmentation Attribute	Accuracy (%)
1	Height and width shift	95.1
2	Rotation	95.3
3	Rotation + Horizontal flip	95.6
4	Rotation + Horizontal flip + Zoom	96.5
5	Rotation + Horizontal and Vertical flip + Zoom	97.7

For the image augmentation process, attributes such as height and width shift, rotation, horizontal flip, and zooming can be performed on the base image dataset. The results of image augmentation on the accuracy of the proposed DenseNet169 method are tabulated in Table 5, and it can be inferred that rotation, horizontal and vertical flip, and zoom lead to the highest model accuracy. This is because of the diversity caused by image augmentation in the training set. Model accuracy for computer vision-related tasks is highly dependent on the diverse nature of the image dataset. With limited training data, the deep learning-based methods fail to capture the learned features and hence result in poor generalization performance.

4.3. Explainable fault detection in wind turbine blades

This section highlights the importance of explainable fault detection in wind turbines, with particular emphasis on rotor blades. Although prior studies demonstrate the effectiveness of machine learning and deep learning approaches for fault

detection and diagnosis, the application of explainability to rotor blade fault detection remains largely unexplored. Explainable fault detection for the turbine blades highlights using interpretable machine learning and deep learning models. In this manuscript, we discuss two popular XAI models, namely, Grad-CAM and SHAP. The idea behind XAI for fault detection is to understand regions/areas of the turbine blade cross-section contributing to a particular damage class. Grad-CAM enhances the interpretability of the neural networks by producing heatmaps that highlight the regions of the input image that influence the final classification decision. The heatmaps so produced, in turn, aid the wind farm operator in understanding the model's failure to capture regions contributing to a classification. This enhances the interpretability of complex models for end users. In summary, the Grad-CAM method utilizes the gradients of the target class score with respect to the final convolutional feature maps to generate visual explanations. his tech-

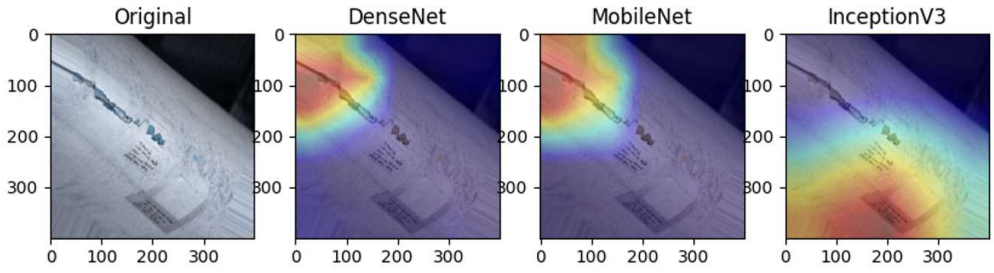


Figure 11: Results of Grad-CAM XAI model Integrated on deep learning models

nique identifies the regions of an input image that exert the greatest influence on the classification outcome. Specifically, regions with higher gradient values indicate areas where the model's final prediction is most dependent on the input data. The Grad-CAM model focuses on a particular instance within the testing dataset to derive probability scores for each class while providing insights into the reasoning behind these assignments. Figure 11 visually presents this prediction process, showcasing the influential features that led to classifying the sample as positive (denoted in blue) or negative (indicated in orange). To enhance transparency, the figure includes a list of feature values associated with the sam-

ple, highlighting their contributions. SHAP (SHapley Additive exPlanations) is a highly significant technique in Explainable Artificial Intelligence (XAI), particularly for image classification models. Offering a dual approach to interpretability, SHAP provides both global and local insights into model predictions. Its unique capability to assign importance scores to individual pixels in an image allows for a granular understanding of each pixel's contribution to the overall decision, providing pixel-level explanations. This feature is especially crucial for discerning influential regions within a turbine blade image and understanding the decision boundaries learned by the model. Moreover, SHAP facilitates model validation and fairness assessment by uncovering potential biases and areas of concern by analyzing pixel impacts on predictions made by deep models. Another advantage is its ability to identify essential regions within an image. It offers crucial insights into where the model focuses its attention during classification, contributing to the interpretability of complex decisions for the wind farm operator. One of SHAP's notable strengths lies in its role in promoting user trust and acceptance of image classification models. By providing interpretable explanations, SHAP addresses the need for transparency and helps wind farm operators comprehend the rationale behind model predictions, ultimately increasing confidence in the model's reliability and, hence, decreasing the potential downtime caused by catastrophic blade damage. Additionally, SHAP values offer a clear and visual means of communicating model results, making it easier to convey intricate decisions to both internal teams and external stakeholders.

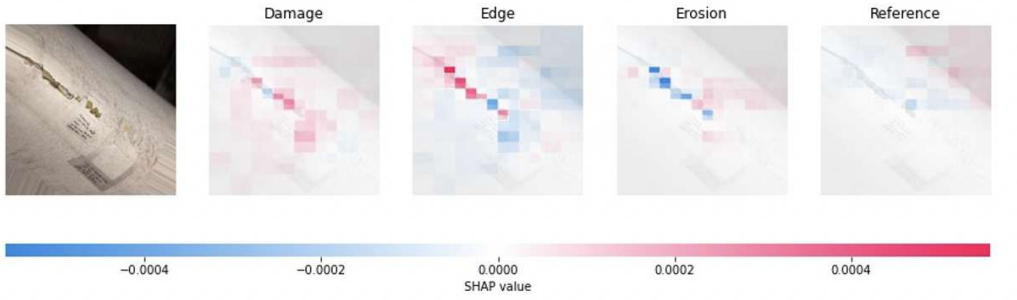


Figure 12: Results of SHAP XAI model Integrated on DenseNet169 deep learning model

Figure 12 shows the representation of the SHAP XAI model that interprets the probability of the class as per the blue and pink identification of the image. In the figure, the Edge class is self-explainable as per the SHAP value, which is neutral in the model. The positive SHAP value positively contributes to the model's prediction for that particular class, and a negative SHAP value negatively contributes to the model's prediction for a given instance. In Figure 12, the pink regions indicate the region of importance for a particular deep learning model, thus aiding the model in predicting the respective class. Thus, the wind farm operators can analyze the sensitive regions based on the SHAP value for a given image and schedule the maintenance procedure accordingly. This is of great importance, as for a 1 MW wind turbine, the rotor blades account for approximately 20-25% of the overall wind turbine cost [42].

4.4. KW-TB-DSS Decision Support

The key contribution of this study lies in the design and implementation of the KW-TB-DSS (Knowledge-Driven Turbine Blade Decision-Support System), which extends beyond deep learning–based classification to provide operator-ready insights for maintenance planning and economic evaluation. Unlike conventional models that deliver only class labels, KW-TB-DSS integrates explainability and decision-support capabilities to transform raw UAV imagery into actionable knowledge.

Interpretable Outputs: The decision-support layer leverages ensemble explainability through Grad-CAM and SHAP fusion, which highlights critical blade regions influencing predictions. These heatmaps, combined with pixel-level importance scores and classification confidence, enable operators to verify and validate the reasoning behind model outputs. This interpretability enhances trust and supports informed decision-making in maintenance workflows.

Operator Actions: By linking interpretable outputs to operational strategies, KW-TB-DSS facilitates maintenance scheduling and compliance monitoring. For example, blades exhibiting severe erosion patterns can be prioritized for immediate inspection or repair, while compliance checks can ensure regulatory standards are

consistently met. This actionable guidance minimizes the reliance on manual inspection alone and accelerates decision cycles.

Economic Implications: From an economic perspective, KW-TB-DSS supports early detection and intervention, thereby reducing turbine downtime and optimizing operational costs. By preventing catastrophic blade failures and extending asset lifetime, the system contributes to overall O&M cost reduction and revenue protection for wind farm operators. The revenue loss due to power reduction is:

$$\Delta R = \Delta P \cdot T \cdot C_{elec}$$

Total O&M cost is:

$$C_{O\&M} = \sum_{i=1}^{N} \left(C^i_{repair} + C^i_{downtime} \right)$$

$$C^i_{downtime} = \Delta P^i \cdot T^i \cdot C_{elec}$$

Figure 13 presents the decision-support layer of KW-TB-DSS. The dashboard aggregates interpretable visualizations (heatmaps, importance scores, confidence values) with recommended operator actions and economic impact indicators, forming a unified interface. This ensures that complex AI-driven analytics are accessible and usable in real-world wind-farm operations.

4.5. Limitations and future directions

While it is insightful to discuss the advantages of the proposed approach for wind turbine blade damage detection, it is only meaningful to point out several limitations. The aerial-imagery-based approach can be jeopardized by adverse weather conditions such as extreme rainfall, fog, and strong winds. In this paper, we have established the robustness of the deep learning approach for damage detection when the input image is blurry, which simulates foggy conditions. It is also vital to have high-resolution cameras mounted on the drone as the poor quality of the images thereof may deter the algorithm from learning representa-

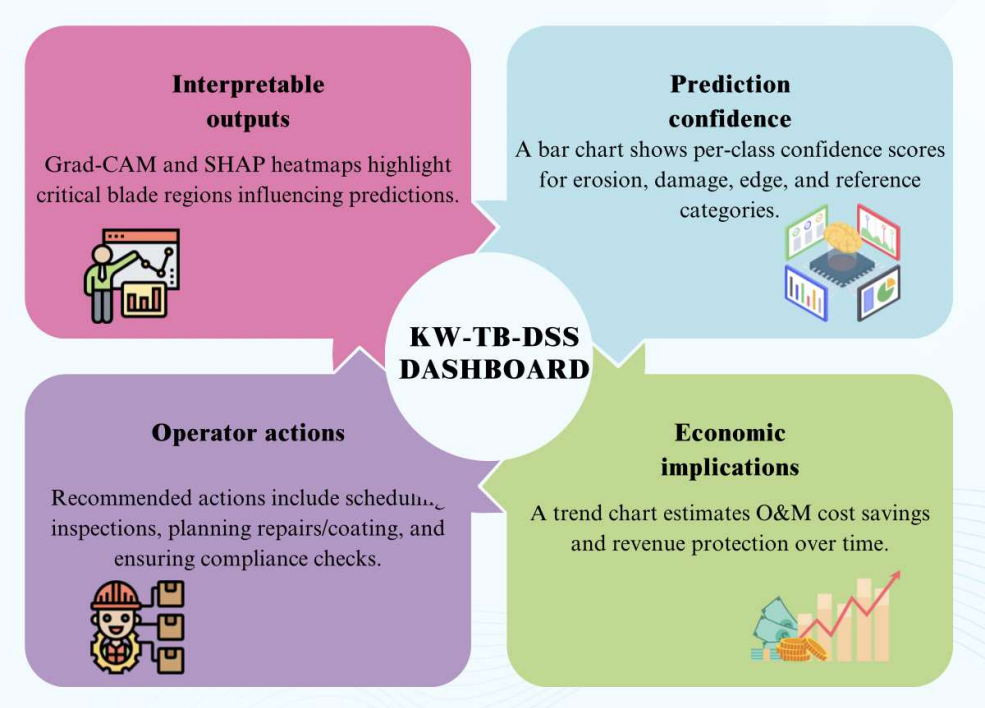


Figure 13: KW-TB-DSS decision-support layer. The dashboard integrates interpretable outputs (Grad-CAM and SHAP heatmaps, importance scores, and confidence values), operator actions (maintenance scheduling, compliance checks), and economic implications (downtime reduction, O&M cost savings) to support reliable wind-farm operations.

tive features. An important direction for extending this work is the integration of uncertainty quantification (UQ) into the explainable fault detection framework. While current results provide interpretability through Grad-CAM and SHAP, they do not explicitly capture how confident the model is in its predictions. In real-world turbine monitoring, this is critical: sensor noise, varying illumination, or blurry images introduce *aleatoric uncertainty*, while limited training samples and unseen fault types lead to *epistemic uncertainty*. Formally, the predictive variance can be decomposed as: Bayesian uncertainty is expressed as:

$$p(y|x) = \int p(y|x,\theta)\, p(\theta|D)\, d\theta$$

Decomposition into aleatoric and epistemic parts:

$$\underbrace{\mathrm{Var}(y|x)}_{\text{Total}} = \underbrace{\mathbb{E}_{\theta\sim p(\theta|D)}[\mathrm{Var}(y|x,\theta)]}_{\text{Aleatoric}} + \underbrace{\mathrm{Var}_{\theta\sim p(\theta|D)}[\mathbb{E}[y|x,\theta]]}_{\text{Epistemic}}$$

Here, the first term represents irreducible noise from the data, while the second term captures model uncertainty due to limited knowledge. Incorporating such decomposition in future iterations of the KW-TB-DSS framework would not only improve trustworthiness but also enable risk-aware decision making for operators, where both the explanation and the associated confidence are available for inspection.

Future research will emphasize remote, online, and real-time detection of turbine blade damage across varying operating conditions. The researchers are willing to investigate further the damage prognosis, defect identification, and interpretation in the near future. The proposed study aims to serve as a reference for understanding damage detection approaches in wind turbine blades, as well as the underlying mechanisms associated with different defect types. It has significance for understanding the research directions and for advancing practical research in the field of wind turbine blade damage detection. Future research thus could be directed toward exploring wind turbine blade damage detection regarding multiple time scales and anomalous operation in the case of grid-connected systems. Regarding uncertainty quantification, the XAI models could be improved after incorporating uncertainty surrounding predictions and input characteristics.

5. Conclusion

In this paper, we introduce KW-TB-DSS (Knowledge-Driven Turbine Blade Decision Support System), an explainable framework for UAV-based wind turbine blade inspection. The system combines deep learning classification with ensemble explainability to transform raw aerial imagery into actionable maintenance knowledge. The paper first discusses wind turbine blade damage detection with a deep learning architecture. Since the initial dataset is highly imbalanced, it is im-

proved by image augmentation, where variation in the dataset is introduced to enhance the deep learning training process. Three algorithms, namely, MobileNet, DenceNet169, and Inception, are considered and yield an accuracy of 95.46%, 97.12% and 96.4%, respectively. Further, to validate the effect of image augmentation on the training data, the accuracy of the proposed DenseNet169 framework is assessed via a sensitivity analysis. Results reveal that horizontal and vertical flip together with zoom and rotation brings out an efficiency of 97.77%. The second part of the paper highlights explainable fault detection for wind turbine blades. Two techniques, namely GradCAM and SHAP, are used to exploit the reasoning power of deep learning for detecting wind turbine blade damage. GradCAM and SHAP highlight crucial regions responsible for predicting a particular damage class, which would aid the wind farm operator in accelerating the maintenance protocol. However, a more generic model that works well with turbines located in different topological regions can be explored for the explainable fault and damage detection in wind turbines. By unifying classification accuracy, explainability, and decision-support capabilities, KW-TB-DSS enables wind farm operators to identify surface damage early, plan maintenance schedules effectively, and mitigate revenue loss. Looking ahead, extending the framework to turbines deployed across diverse geographical and environmental conditions will further advance its role as a scalable and reliable decision-support system for wind-farm operations.

Ethics Approval

No human subjects or animals are involved in the research.

Consent to Participate:

All authors have mutually consented to participate.

Consent to Publish:

All the authors have consented to the Journal publishing this paper.

Data Availability Statement:

All data generated or analysed during this study are provided by the corresponding author on reasonable request.

Funding Statement:

The authors received no specific funding for this study.

Conflicts of Interest:

The authors declare that they have no conflicts of interest to report regarding the present study.

Declaration

Results are accurately reported, any overstated conclusions are rewritten, and the limitations of the work fully explained.

Author contributions statement

All authors (Madhuri Gupta, Harsh S. Dhiman, Sameer Malik, Achyut Shankar, Wattana Viriyasitavat, Jaydeep Kishore, Sonu Kumar Das) contributed equally.

References

[1] S.-X. Lv and L. Wang, "Deep learning combined wind speed forecasting with hybrid time series decomposition and multi-objective parameter optimization," *Applied Energy*, vol. 311, p. 118674, Apr. 2022.

[2] H. S. Dhiman, D. Deb, and J. M. Guerrero, "Hybrid machine intelligent SVR variants for wind forecasting and ramp events," *Renewable and Sustainable Energy Reviews*, vol. 108, pp. 369–379, Jul. 2019.

[3] B. Lu, Y. Li, X. Wu, and Z. Yang, "A review of recent advances in wind turbine condition monitoring and fault diagnosis," in *2009 IEEE Power Electronics and Machines in Wind Applications*, pp. 1–7, 2009.

[4] H. S. Dhiman, D. Deb, S. M. Muyeen, and I. Kamwa, "Wind turbine gearbox anomaly detection based on adaptive threshold and twin support vector machines," *IEEE Transactions on Energy Conversion*, pp. 1–1, 2021.

[5] Z. Qiu, S. Wang, Z. Zeng, and D. Yu, "Automatic visual defects inspection of wind turbine blades via YOLO-based small object detection approach," *J. Electron. Imaging*, vol. 28, p. 1, Aug. 2019.

[6] J. P. Amezquita-Sanchez and H. Adeli, "Signal processing techniques for vibration-based health monitoring of smart structures," *Archives of Computational Methods in Engineering*, vol. 23, pp. 1–15, Oct. 2014.

[7] A. Abouhnik and A. Albarbar, "Wind turbine blades condition assessment based on vibration measurements and the level of an empirically decomposed feature," *Energy Conversion and Management*, vol. 64, pp. 606–613, Dec. 2012.

[8] L. Yang and Z. Zhang, "Wind turbine gearbox failure detection based on SCADA data: A deep learning-based approach," *IEEE Transactions on Instrumentation and Measurement*, vol. 70, pp. 1–11, 2021.

[9] L. Lu, Y. He, Y. Ruan, and W. Yuan, "Wind turbine planetary gearbox condition monitoring method based on wireless sensor and deep learning approach," *IEEE Transactions on Instrumentation and Measurement*, vol. 70, pp. 1–16, 2021.

[10] V. Vapnik, "An overview of statistical learning theory," *IEEE Transactions on Neural Networks*, vol. 10, no. 5, pp. 988–999, 1999.

[11] S. Marsland, *Machine Learning*, Chapman and Hall/CRC, Oct. 2014.

[12] R. Rao, "Reinforcement learning; an introduction r.s. sutton, a.g. barto (eds.); MIT press, cambridge, MA, 1998, 380 pages, ISBN 0-262-19398-1, $42.00," *Neural Networks*, vol. 13, pp. 133–135, Jan. 2000.

[13] H. S. Dhiman, D. Deb, J. Carroll, V. Muresan, and M.-L. Unguresan, "Wind turbine gearbox condition monitoring based on class of support vector regression models and residual analysis," *Sensors*, vol. 20, p. 6742, Nov. 2020.

[14] M. Catelani, L. Ciani, D. Galar, and G. Patrizi, "Optimizing maintenance policies for a yaw system using reliability-centered maintenance and data-driven condition monitoring," *IEEE Transactions on Instrumentation and Measurement*, vol. 69, pp. 6241–6249, Sept. 2020.

[15] R. Pandit, D. Infield, and T. Dodwell, "Operational variables for improving industrial wind turbine yaw misalignment early fault detection capabilities using data-driven techniques," *IEEE Transactions on Instrumentation and Measurement*, vol. 70, pp. 1–8, 2021.

[16] C. G. Mun~oz and F. G. M´arquez, "A new fault location approach for acoustic emission techniques in wind turbines," *Energies*, vol. 9, p. 40, Jan. 2016.

[17] K.-Y. Oh, J.-Y. Park, J.-S. Lee, B. I. Epureanu, and J.-K. Lee, "A novel method and its field tests for monitoring and diagnosing blade health for wind turbines," *IEEE Transactions on Instrumentation and Measurement*, pp. 1–1, 2015.

[18] W. Yang, Z. Lang, and W. Tian, "Condition monitoring and damage location of wind turbine blades by frequency response transmissibility analysis," *IEEE Transactions on Industrial Electronics*, vol. 62, pp. 6558–6564, Oct. 2015.

[19] M. Moradi and S. Sivoththaman, "MEMS multisensor intelligent damage

detection for wind turbines," *IEEE Sensors Journal*, vol. 15, pp. 1437–1444, Mar. 2015.

[20] M. Stokkeland, K. Klausen, and T. A. Johansen, "Autonomous visual navigation of unmanned aerial vehicle for wind turbine inspection," in *2015 International Conference on Unmanned Aircraft Systems (ICUAS)*, IEEE, Jun 2015.

[21] C. Kanellakis, E. Fresk, S. S. Mansouri, D. Kominiak, and G. Nikolakopoulos, "Towards visual inspection of wind turbines: A case of visual data acquisition using autonomous aerial robots," *IEEE Access*, vol. 8, pp. 181650–181661, 2020.

[22] F. Bu and M. S. Gharajeh, "Intelligent and vision-based fire detection systems: A survey," *Image and Vision Computing*, vol. 91, p. 103803, Nov. 2019.

[23] L. Wang, Z. Zhang, and X. Luo, "A two-stage data-driven approach for image-based wind turbine blade crack inspections," *IEEE/ASME Transactions on Mechatronics*, vol. 24, pp. 1271–1281, Jun. 2019.

[24] D. Astolfi, F. De Caro, and A. Vaccaro, "Condition Monitoring of Wind Turbine Systems by Explainable Artificial Intelligence Techniques," *Sensors*, vol. 23, no. 12, pp. 5376, 2023.

[25] Chatterjee, J., & Dethlefs, N. (2020). Deep learning with knowledge transfer for explainable anomaly prediction in wind turbines. *Wind Energy*, 23(8), 1693-1710.

[26] Kim, D. Y., & Kim, B. S. (2023). Contribution of meteorological factors based on explainable artificial intelligence in predicting wind farm power production using machine learning algorithms. *Journal of Renewable and Sustainable Energy*, 15(1).

[27] Chatterjee, J. (2020, August). Explainable AI for Intelligent Decision Support in Operations & Maintenance of Wind Turbines. In 1st Doctoral Consortium at the European Conference on Artificial Intelligence (DC-ECAI 2020) (Vol. 29, No. 5000, p. 6000).

[28] Chatterjee, J., & Dethlefs, N. (2020, September). Temporal causal inference in wind turbine SCADA data using deep learning for explainable AI. In *Journal of Physics: Conference Series* (Vol. 1618, No. 2, p. 022022). IOP Publishing.

[29] Chatterjee, J., & Dethlefs, N. (2020). XAI4Wind: A multimodal knowledge graph database for explainable decision support in operations & maintenance of wind turbines. arXiv preprint arXiv:2012.10489.

[30] Attallah, O., Ibrahim, R. A., & Zakzouk, N. E. (2022). Fault diagnosis for induction generator-based wind turbine using ensemble deep learning techniques. *Energy Reports*, 8, 12787-12798. Elsevier.

[31] Liu, Y., Wang, Z., Wu, X., Fang, F., & Saqlain, A. S. (2023). Cloud-Edge-End Cooperative Detection of Wind Turbine Blade Surface Damage Based on Lightweight Deep Learning Network. *IEEE Internet Computing*, 27(1), 43-51. DOI: 10.1109/MIC.2022.3175935

[32] Zhang, C., Wen, C., & Liu, J. (2020). Mask-MRNet: A deep neural network for wind turbine blade fault detection. *Journal of Renewable and Sustainable Energy*, 12(5). AIP Publishing.

[33] K. Simonyan and A. Zisserman, "Very deep convolutional networks for large-scale image recognition," 2015.

[34] Z. Song, L. Fu, J. Wu, Z. Liu, R. Li, and Y. Cui, "Kiwifruit detection in field images using faster R-CNN with VGG16," *IFAC-PapersOnLine*, vol. 52, no. 30, pp. 76–81, 2019.

[35] A. Krizhevsky, I. Sutskever, and G. E. Hinton, "Imagenet classification with deep convolutional neural networks," in *Proceedings of the 25th International Conference on Neural Information Processing Systems-Volume 1*, NIPS'12, (Red Hook, NY, USA), p. 1097–1105, Curran Associates Inc., 2012.

[36] R. R. Selvaraju, M. Cogswell, A. Das, R. Vedantam, D. Parikh, and D. Batra, "Grad-CAM: Visual Explanations from Deep Networks via Gradient-Based Localization," *2017 IEEE International Conference on Computer Vision (ICCV)*, Venice, Italy, 2017, pp. 618-626, doi: 10.1109/ICCV.2017.74.

[37] M. A. Ganaie and M. Hu, "Ensemble deep learning: A review," *arXiv.org*, 2021. [Online]. Available: https://arxiv.org/abs/2104.02395.

[38] T. C. Lin and H. C. Lee, "Skin cancer Dermoscopy Images classification with meta data via deep Learning Ensemble," *2020 International Computer Symposium (ICS)*, pp. 237-241, 2020.

[39] R. Liu et al., "Ensemble learning with MULTICLASSIFIERS on Pediatric Hand RADIOGRAPH segmentation for Bone Age Assessment," *International Journal of Biomedical Imaging*, vol. 2020, pp. 1–12, 2020.

[40] I. Nikolov, "Wind turbine blade surfaces dataset," *Mendeley*, 2020.

[41] Flusser, J., Farokhi, S., Höschl, C., Suk, T., Zitova, B., & Pedone, M. (2015). Recognition of images degraded by Gaussian blur. *IEEE Transactions on Image Processing*, 25(2), 790-806.

[42] Bortolotti, P., Berry, D. S., Murray, R., Gaertner, E., Jenne, D. S., Damiani, R. R., ... & Dykes, K. L. (2019). A detailed wind turbine blade cost model (No. NREL/TP-5000-73585). National Renewable Energy Lab.(NREL), Golden, CO (United States).